Journal of Biomolecular NMR, **13:** 43–50, 1999.
KLUWER/ESCOM

Half-filter experiments for assignment, structure determination and hydration analysis of unlabelled ligands bound to $^{13}C/^{15}N$ labelled proteins

Claudio Dalvit*, Sylvain Cottens, Paul Ramage & Ulrich Hommel
NOVARTIS Pharma AG, CH-4002 Basel, Switzerland

Received 7 August 1998; Accepted 16 September 1998

Key words: 1D, 2D and 3D $^{13}C/^{15}N$ ω_2 half-filter experiments, LFA-1, ligand hydration, pulsed field gradients

Abstract

A novel variant of the $^{13}C/^{15}N$ ω_2 half-filter experiment is reported for studying the hydration of an unlabelled ligand bound to a ^{15}N and ^{13}C uniformly labelled biological macromolecule. This doubly tuned filter experiment represents a powerful tool for obtaining resonance assignments, structure determination and hydration properties of a ligand. Its application to the binary complex formed by the inserted-domain (I-domain) of the leukocyte function-associated antigen-1 (LFA-1) with a ligand reveals the presence of H_2O molecules at the binding interface.

Introduction

Water plays a pivotal role in the protein-ligand, protein-DNA and protein-protein recognition mechanism. Several structural studies based on X-ray and NMR spectroscopy have identified water molecules at the interfaces of macromolecular complexes (Chuprina et al., 1993; Qian et al., 1993; Bath et al., 1994; Clore et al., 1994; Braden et al., 1995). The contribution of the displacement and/or burial of these H_2O molecules to the thermodynamic and energetic ligand-protein assembly has been the subject of recent theoretical investigations. The entropically favourable liberation of water from an hydrophobic cavity is associated with enthalpically unfavourable effects deriving from the breaking of H_2O-H_2O and protein-H_2O bonds (Renzoni et al., 1997). Therefore, there is a balance between the compensatory effects of entropy and enthalpy. However, recently it has been demonstrated that for weakly hydrogen-bonded water molecules in crevices on the protein surface the water displacement may well be accompanied by an entropy loss (Denisov et al., 1997).

A rational design of the ligand aimed at optimizing the favourable enthalpy of H_2O molecules at the interface between receptor and ligand can yield a novel inhibitor with improved binding affinity. Thus, a better understanding of the structural and dynamic properties of water molecules at the binding interface provide important information for the purpose of drug design.

Recently, NMR spectroscopy has emerged as a potent technique for the identification of H_2O molecules bound to the interior of biological macromolecules in solution (Otting et al., 1989a, 1991; Clore et al., 1990; Grzesiek and Bax, 1993; Kriwacki et al., 1993; Mori et al., 1994, 1996; Dalvit and Hommel, 1995; Dötsch and Wider, 1995; Otting and Liepinsh, 1995; Birlirakis et al., 1996; Böckmann and Guittet, 1996; Dalvit, 1996; Wider et al., 1996; Hwang et al. 1997). We propose here a variant of the $^{13}C/^{15}N$ ω_2 half-filter NMR experiment which allows sensitive measurement of the hydration of an unlabelled ligand complexed with a ^{15}N and/or ^{13}C uniformly labelled biological macromolecule. Application of this technique to the binary complex formed by the inserted-domain (I domain) of the leukocyte function-associated antigen (LFA-1) with a low molecular weight ligand reveals the presence of H_2O molecules at the binding interface. Implementation of this new variant of the $^{13}C/^{15}N$ ω_2 half-filter scheme into 2D and 3D experiments allows one, similar to other filter experiments published in the literature, to obtain resonance assignments and to determine the 3D structure of an unlabelled ligand bound to a $^{13}C/^{15}N$ labelled protein dissolved in H_2O.

*To whom correspondence should be addressed.

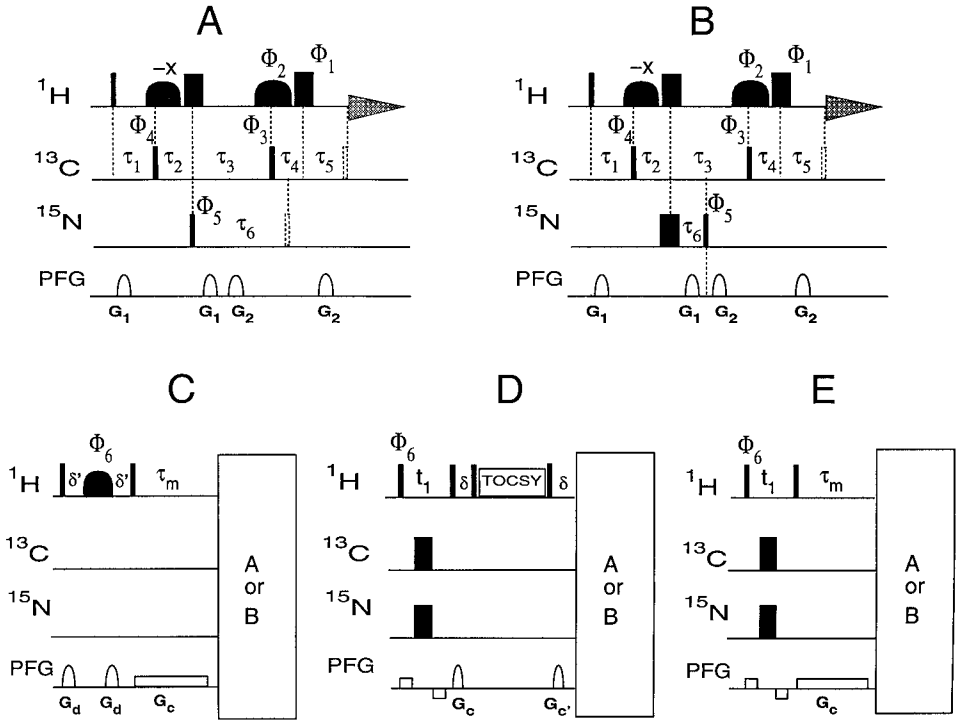

Figure 1. A, B. Pulse sequences of two different $^{13}C/^{15}N$ ω_2 half-filter schemes and their incorporation in the ePHOGSY-NOE (C), TOCSY (D) and NOESY (E) experiments. Narrow and wide bars correspond to 90° and 180° hard pulses, respectively. The two H_2O selective 180° pulses of the detection scheme are either rectangular or strongly truncated Gaussian pulses for better selectivity. The H_2O selective 180° pulse in (C) is a Gaussian pulse of length 30–50 ms. This pulse is flanked by two gradients G_d of equal sign and strength. The delay δ' is equal to the length of the gradient plus a gradient recovery time, but, if necessary, it can be set to longer values for T_2-filtering out the broad signals resonating at the H_2O chemical shift. The phases are in (A,B) ϕ_1 = (x, −y, −x, y); ϕ_2 = (−x, y, x, −y); ϕ_3 = 8(x), 8(−x); ϕ_4 = 4(x), 4(−x); ϕ_5 = 16(x), 16(−x); ϕ_{rec} = (x, −x); in (C) ϕ_1 = 4(x), 4(−y), 4(−x), 4(y); ϕ_2 = 4(−x), 4(y), 4(x), 4(−y); ϕ_3 = 32 (x), 32(−x); ϕ_4 = 16(x), 16(−x); ϕ_5 = 64(x), 64(−x); ϕ_6 = (x, −y, −x, y); ϕ_{rec} = 2(x, −x), 2(−x, x); in (D,E) ϕ_1 = 2(x), 2(−y), 2(−x), 2(y); ϕ_2 = 2(−x), 2(y), 2(x), 2(−y); ϕ_3 = 16(x), 16(−x); ϕ_4 = 8(x), 8(−x); ϕ_5 = 32(x), 32(−x); ϕ_6 = (x, −x); ϕ_{rec} = (x, −x, −x, x). The phases of the other pulses are x unless otherwise indicated. If the second 90° ^{15}N pulse is applied this is also phase cycled +x and −x. Quadrature detection in the t_1 dimension is obtained by changing ϕ_6 in (D,E) in the regular TPPI manner (Marion and Wüthrich, 1983). The length of the H_2O selective 180° pulses, the length of the gradients plus the gradient recovery time and the different delays are chosen for optimal minimization of Equation 1 and for suppression of ^{15}N-bound proton resonances. The first ^{15}N 90° pulse is applied 5.3–5.4 ms after the ^1H 90° pulse. The second ^{15}N 90° pulse which is optional is set at a delay of 5.3–5.4 ms after the first 180° ^1H hard pulse. The delay τ_5 is equal to the length of the PFG plus the gradient recovery time. The use of the 3rd ^{13}C 90°pulse immediately before acquisition is discussed in the text. If only suppression of protons bound to ^{13}C nuclei is desired it is sufficient to remove the ^{15}N pulses. Furthermore the delay $\tau_1 + \tau_2$ (and consequently $\tau_3 + \tau_4$) can be set to a shorter value. The gradient G_c in (C) and (E) is a weak rectangular PFGs applied for the entire length of the mixing time τ_m. This PFG is followed by a gradient recovery time of typically 1 ms before application of the next ^1H 90° pulse. A weak bipolar PFG is applied during the evolution period t_1 (Sklenár, 1995) in (D) and (E). The delay δ in (D) corresponds to the length of the gradients G_c plus a gradient recovery time of 100–200 μs.

Materials and methods

The system chosen for application of the novel technique is represented by an aqueous solution of a protein-ligand complex. The concentration of the complex was 0.6 mM. The sample is in phosphate buffered saline (PBS), pH 7.0, and contains 10 mM $MgSO_4$. The ^{13}C and ^{15}N uniformly labelled protein is the I domain of LFA-1 consisting of 188 amino acids. The ligand is a low molecular weight synthetic compound. The molar ratio of the protein-ligand was 1:1. The affinity of the ligand for the protein is in the low micromolar range. This is judged on the presence of intermediate exchange phenomena observed for protein resonances affected by ligand binding. All experiments have been recorded at T = 296 K with a 600 MHz spectrometer comprising a Bruker actively shielded magnet and an Avance Bruker console. The gradients were generated with an ACCUSTAR^{TM} unit connected to a 5 mm triple-resonance inverse probe.

Results and discussion

Several versions of the $^{13}C/^{15}N$ ω_2 half-filter experiment have been proposed in the literature (Otting and Wüthrich, 1989b, 1990; Wider et al., 1990; Gemmecker et al., 1992; Ikura and Bax, 1992; Petros et al., 1992; Lee et al., 1993, 1994; Bax et al., 1994; Folmer et al., 1995; Ogura et al., 1996; Zwahlen et al., 1997). A novel variant of this type of experiments for recording spectra in aqueous solutions is shown in Figures 1A and 1B. The detection scheme is based on the excitation sculpting sequence (Hwang and Shaka, 1995). The pulse sequence achieves efficient simultaneous suppression of the H_2O signal and of the resonances of protons bound to ^{13}C and ^{15}N nuclei. The purging is obtained by conversion of proton heteronuclear antiphase magnetization to heteronuclear Multiple-Quantum (MQ) coherence (Kogler et al., 1983). The combination of gradients dephases completely the magnetization which has followed this coherence pathway (Keeler et al., 1994) and consequently is not visible. The amount of residual in-phase and anti-phase magnetization of a proton I bound to ^{13}C (S) at the end of the scheme of Figure 1 is proportional to:

$$I_y \propto \cos\pi J_{IS}\tau_1 \cos\pi J_{IS}(\tau_3 - \tau_2) \cos\pi J_{IS}(\tau_5 - \tau_4) \quad (1)$$

$$2I_xS_z \propto \cos\pi J_{IS}\tau_1 \cos\pi J_{IS}(\tau_3 - \tau_2) \sin\pi J_{IS}(\tau_5 - \tau_4) \quad (2)$$

where J_{IS} is the heteronuclear one bond coupling constant and the different delays are depicted in Figure 1. Suppression of the ^{13}C-bound proton signals is performed, according to Equations 1 and 2, by properly tuning the length of the delays τ_1 and $(\tau_3 - \tau_2)$.

The former is set equal to $1/(2^1J_{CH})$ and the latter to $1/(2^1J'_{CH})$ where $^1J_{CH}$ and $^1J'_{CH}$ are two different one bond heteronuclear coupling constants. The dispersive anti-phase term of Equation 2 is smaller compared to the in-phase term of Equation 1 because the delay $(\tau_5 - \tau_4)$ is short. Nevertheless, this heteronuclear anti-phase magnetization can be made unobservable by simply applying a third 90° ^{13}C pulse after τ_5 and immediately before the acquisition period as depicted in Figure 1. The delay $(\tau_1 + \tau_2)$ which is equal to the length of the PFG plus the gradient recovery time and plus the length of the H_2O selective 180° pulse is set to $1/(2^1J_{NH})$ ($\approx$ 5.4 ms) for suppression of the ^{15}N-bound proton signals. The H_2O selective 180° pulses are rectangular or strongly truncated Gaussian pulses of typical length 4 to 4.4 ms.

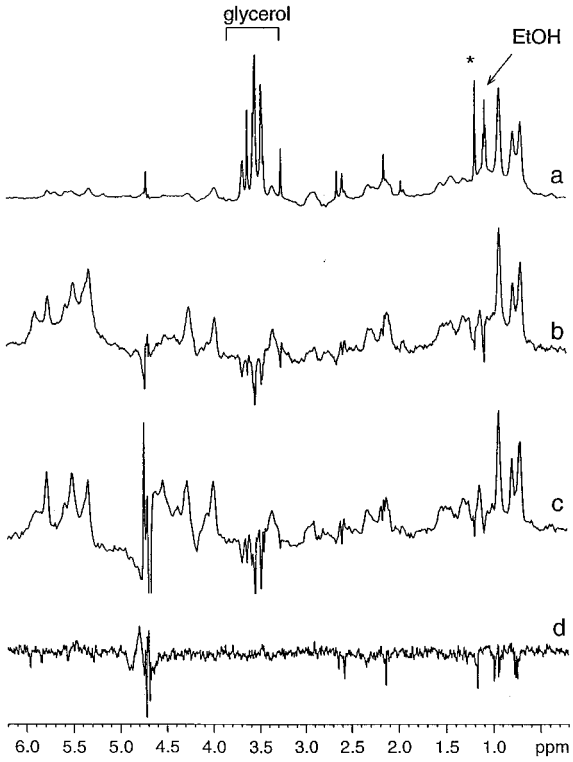

Figure 2. One-dimensional $^{13}C/^{15}N$ ω_2 half-filter reference spectrum (a) and ePHOGSY spectrum (b) recorded with the schemes of Figure 1A and Figure 1C (with filter A), respectively. (c) Cross-section taken at the H_2O ω_1 frequency from the 2D ^{15}N and ^{13}C ω_2 half-filter NOESY experiment recorded with the scheme of Figure 1E (with filter A). The sample is a 0.6 mM aqueous solution (5% D_2O) of the ^{13}C, ^{15}N labelled LFA-1 protein complexed with a low molecular weight synthetic compound. (d) One-dimensional ePHOGSY-NOE spectrum recorded for the ligand alone dissolved in PBS. A total of 64 (a), 8192 (b), 30400 (c) and 4096 (d) scans were recorded. The length of the two H_2O selective rectangular 180° pulses was 4.4 ms in all experiments. The length of the first H_2O selective 180° pulse in (b) was 36 ms. The gradients G_1 and G_2 and the gradient recovery time were 800 and 200 μs long, respectively. The delay τ_1, τ_2, τ_3, τ_4 and τ_5 were 2.9 ms (2.8 ms in A), 2.5 ms, 6.39 ms, 10 μs, 1 ms, respectively. Note that with this combination of PFGs, value of τ_1 tuned to the $^1J_{CH}$ of aromatic protons and length of H_2O selective 180° pulses, the suppression of aliphatic protons is achieved with τ_4 almost equal to 0 in agreement with Equation 1. If instead the value of τ_1 is tuned to the $^1J_{CH}$ of aliphatic protons then the suppression of aromatic protons is achieved with a longer τ_4. The length of the mixing time in (b–d) was 200 ms and the repetition time was 2.25s. Similar results were obtained with τ_m = 100 ms. The gradients G_1 and G_2 had sine-shape and the gradient G_c had a rectangular shape. The gradient strength for G_d, G_c, G_1 and G_2 was about 7, 0.2, 6, 16 G/cm, respectively. The digital resolution in (b) and (c) is 1 and 7 Hz per point, respectively. The asterisk in (a) indicates an impurity of the ligand.

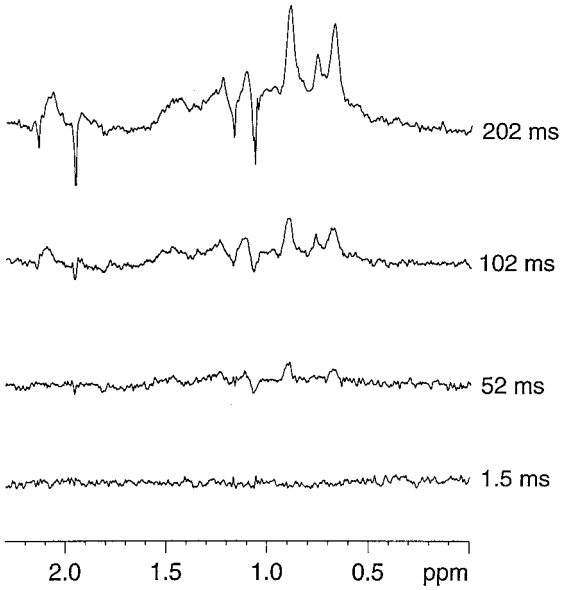

Figure 3. One-dimensional $^{13}C/^{15}N$ ω_2 half-filter ePHOGSY NOE spectra recorded with the scheme of Figure 1C (with filter A). The length of the mixing time is indicated on the spectra. All other experimental parameters are the same as described in Figure 2b. Note the complete absence of artefacts in the spectrum recorded with the shortest mixing time.

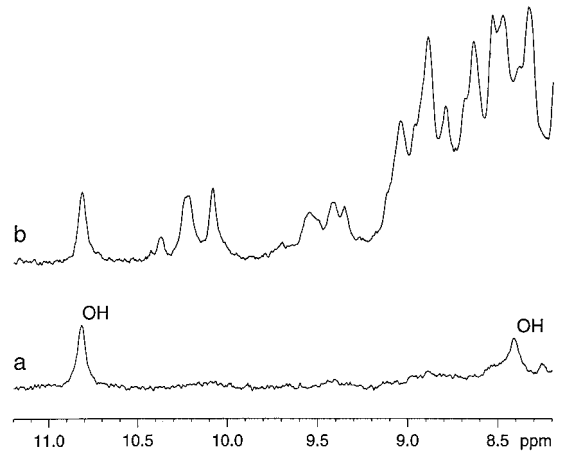

Figure 4. A section of the amide spectral region extracted from 1D ePHOGSY NOE spectra recorded with (a) and without the $^{13}C/^{15}N$ ω_2 half-filter scheme. The mixing time was 202 ms in both experiments. All the other experimental parameters are the same as described in Figure 2b. The two peaks in (a) originating from chemical exchange between OH protons of the protein and H_2O are labelled.

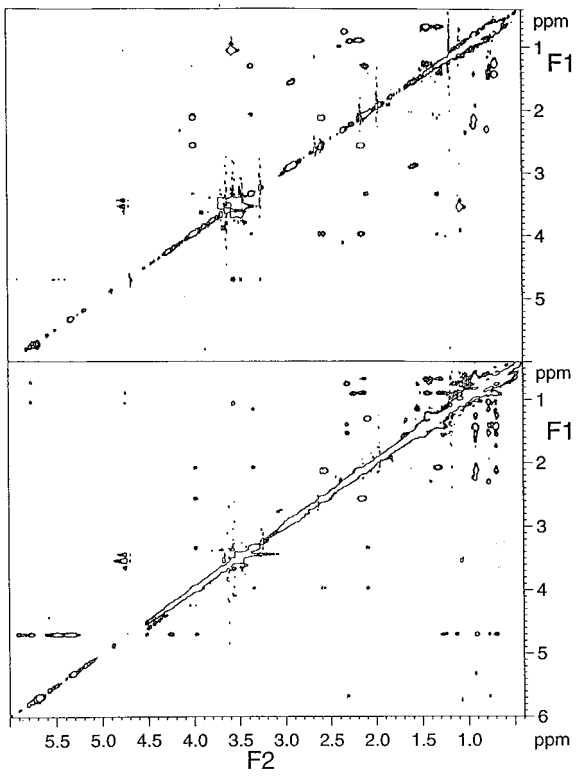

Figure 5. Two-dimensional $^{13}C/^{15}N$ ω_2 half-filter TOCSY (upper trace) and NOESY (lower trace) spectra recorded for the binary complex with the pulse sequence of Figure 1D and 1E (with filter A), respectively. A total of 64 scans (upper trace) with repetition time 1.14 s and 128 scans (lower trace) with repetition time 1.54 s were recorded for each of the 320 t_1 increments. The number of points for t_2 was 2048. The spectral width in ω_1 and ω_2 was 12 ppm. The data were multiplied with a cosine window function prior to Fourier transformation. The lengths of the WALTZ-16 (Shaka et al., 1983) isotropic mixing period and of the mixing period of the NOESY were 38 and 102 ms, respectively. The parameters for the filter are the same as described in Figure 2.

The selectivity of these pulses is sufficient and resonances very close to the H_2O signal can be observed. Computer simulations indicate that for example the use of a 4.4 ms rectangular 180° pulse yields signal attenuation of more than 50% in a narrow bandwidth of only ±114 Hz centered at the H_2O frequency. The suppression of multiple solvent signals is also possible with the schemes of Figure 1 by simply replacing the H_2O soft 180° pulse with a soft 180° shifted laminar pulse having excitation at the different solvent signal frequencies.

When high selectivity is not required, the purging sequence of Figure 1B can also be used. The 180° H_2O selective pulses are stronger and the total duration of the scheme is 2–3 ms shorter compared to the

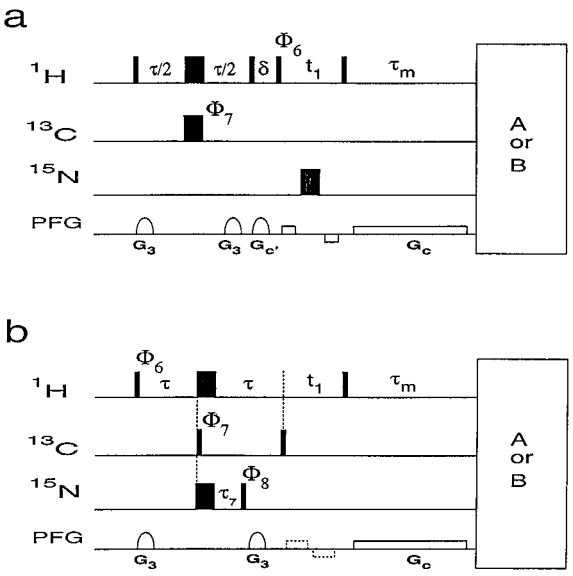

Figure 6. Pulse sequences for the 2D $^{13}C/^{15}N$ ω_2 half-filter NOESY with a ^{13}C ω_1 filter (a) and with a $^{13}C/^{15}N$ ω_1 filter (b). Narrow and wide bars correspond to 90° and 180° hard pulses, respectively. The delays τ and τ_7 are equal to 3.4 and 2 ms, respectively. The phases are ϕ_6 = (x, −x); ϕ_7 = 64(x), 64(−x); ϕ_8 = 128(x), 128(−x). If necessary a z-filter can be used also in (b). All other phases are the same as described in Figure 1E. For the experimental parameter of the box A or B see Figure 1. Quadrature detection in t_1 is obtained with the TPPI method.

scheme of Figure 1A. The ^{15}N 90° pulse is moved between the second and third PFG and an additional ^{15}N 180° pulse is applied simultaneously to the first ^{1}H hard 180° pulse (Ikura and Bax, 1992). The delay $(\tau_1 + \tau_2 + \tau_6)$ is set equal to $1/(2^1J_{NH})$ ($\approx$5.4 ms) for suppression of the ^{15}N-bound proton signals. In our experience this scheme does not provide the same excellent ^{15}N-H resonance suppression as the scheme of Figure 1A. This is probably due to imperfections of the ^{15}N 180° pulse. Nevertheless, this scheme represents an alternative to the scheme of Figure 1A and can be applied in the 2D and 3D versions of the $^{13}C/^{15}N$ ω_2 half-filter experiment.

Implementation of the schemes of Figure 1A and Figure 1B in the one-dimensional ePHOGSY experiment (Dalvit and Hommel, 1995; Dalvit, 1996) is shown in Figure 1C. This experiment selects only the water magnetization transferred to the unlabelled ligand via cross-relaxation and/or chemical exchange. Extension of this scheme to two-dimensions is straightforward as shown previously (Dalvit, 1996). Finally, Figure 1D and 1E show the insertion of the filter in the 2D TOCSY and NOESY experiments, respectively, for the assignment and structure determination of a ligand bound to a protein.

The one-dimensional spectrum recorded for the binary complex $^{13}C/^{15}N$ LFA-1-ligand with the pulse sequence of Figure 1A is shown in Figure 2a. The broad resonances observed in this spectrum originate mostly from the protons of the ligand and from the OH protons of the protein. However, due to the non-complete ^{13}C labelling of the protein (95% ^{13}C labelling), some very weak protein ^{12}C-bound proton signals are also observed. In addition, all the sharp resonances originating from traces of ethanol, glycerol and another impurity present in the ligand solution are also observed in this spectrum. The linewidth of the ligand CH_3 resonances is of the same magnitude (FWHH = 25–30 Hz) as the linewidth of the protein CH_3 resonances and no multiplet fine structure can be resolved. This indicates that the ligand forms a tight complex with the protein. The same spectral region of the experiment recorded with the scheme of Figure 1C and 1E (cross section taken at the H_2O ω_1 frequency) are shown in Figure 2b and 2c, respectively. These two spectra are almost identical, indicating that the two experiments provide the same results. The small differences are simply due to the different digital resolution of the two spectra. The only real difference is the superior sensitivity of the ePHOGSY experiment. This is easily explained by the fact that the desired H_2O-ligand NOE signals are recorded in every scan of the ePHOGSY experiment whereas these signals are detected in only half of the total number of scans of the 2D NOESY experiment. The one-dimensional ePHOGSY-NOE experiment recorded for the ligand alone is shown in Figure 2d. The resonances in Figures 2b, 2c located downfield from H_2O originate mostly from chemical exchange between H_2O and the hydroxyl protons of serine and threonine residues. It is noteworthy that although these resonances are close to the H_2O signal they can be easily observed. The intermolecular NOEs between H_2O and the molecules ethanol and glycerol which do not interact with the protein are negative ($\sigma > 0$). These NOEs are due predominantly to a relay process via the OH protons. On the contrary, the NOEs between H_2O and several protons of the ligand are negative ($\sigma > 0$) for the ligand solution (Figure 2d) and are positive ($\sigma < 0$) for the binary complex solution (Figures 2b and 2c). Figures 3a–d show four one-dimensional $^{13}C/^{15}N$ ω_2 half-filter ePHOGSY spectra recorded with different mixing times. The NOEs between H_2O and ligand are observed even at short mixing times indicating

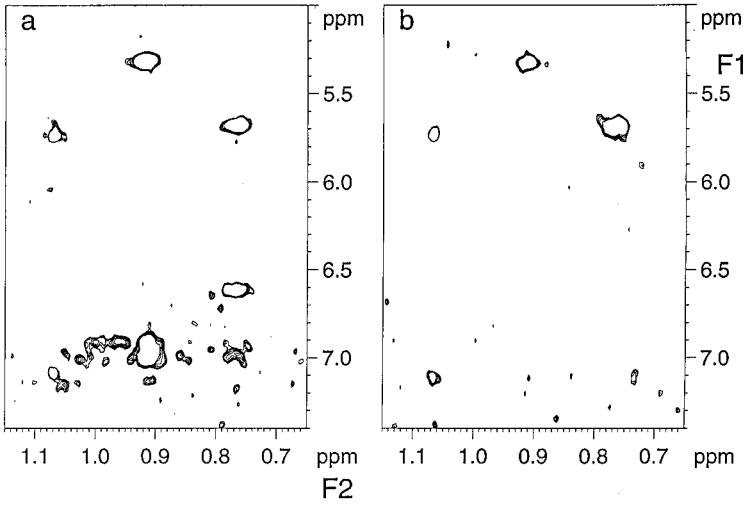

Figure 7. An expanded region of the 2D $^{13}C/^{15}N$ ω_2 half-filter NOESY spectra without (a) and with (b) a ^{13}C ω_1 filter. The experiments have been recorded for the binary complex with the pulse sequences of Figures 1E and 6a, respectively. The filter A was used for both experiments. A total of 128 scans with a repetition time 1.54 s were recorded for each of the 320 t_1 increments. In (b) the delay $\tau/2$, the first two gradients and their gradient recovery time were 1.7, 0.5 and 0.2 ms long, respectively. All other parameters are the same as described in Figure 5.

that these effects are not due to spin diffusion, but represent direct interactions between H_2O and ligand. The $^{13}C/^{15}N$ ω_2 half-filter ePHOGSY spectrum recorded with a very short mixing time does not have any signal. This is an important finding which demonstrates that the ePHOGSY spectra do not contain any of those artefacts originating from the effect of radiation damping and/or demagnetizing field (Sobol et al., 1998).

The positive intermolecular NOEs between H_2O and protons of the ligand when complexed to the protein can be explained with the presence of water molecules at the interface between protein and ligand. The lifetime of this bound H_2O has to be longer than ~ 1 ns (Otting et al., 1991). Our studies indicate that several protons of the ligand are close in space to these H_2O molecules. Some of these protons belong to the hydrophobic moiety of the ligand. Preliminary structural inspection of the protein-ligand complex excludes the possibility that the observed NOEs stem from a relay process via OH protons of either protein or ligand. A detailed structural analysis of these interactions must await the full structure determination of the protein-ligand complex. In addition to the ^{13}C-bound proton resonance suppression the filter achieves also excellent ^{15}N-bound proton resonances suppression. This can be appreciated in Figure 4 which shows a section of the amide spectral region extracted from ePHOGSY spectra recorded with (a) and without (b) $^{13}C/^{15}N$ ω_2 half-filter scheme. All the NH

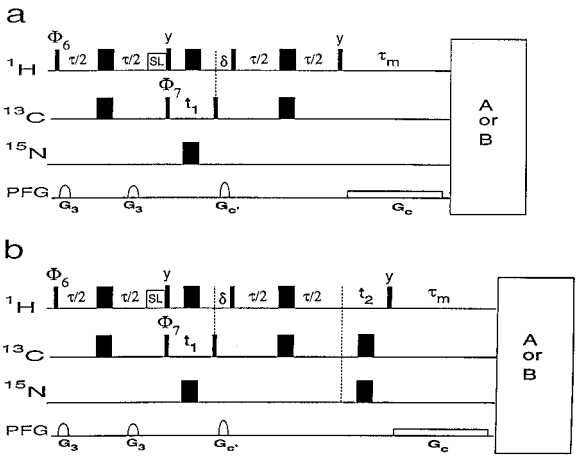

Figure 8. Pulse sequences for the 2D (a) and 3D (b) ^{13}C ω_1 edited and ^{13}C /^{15}N half-filter (in the acquisition dimension) experiment. Narrow and wide bars correspond to 90° and 180° hard pulses, respectively. The delay $\tau/2$ is equal to 1.7 ms. The phases are ϕ_6 = 64(x), 64(−x); ϕ_7 = (x, −x); ϕ_{rec} = 16(x, −x, −x, x), 16(−x, x, x, −x). All other phases are the same as described in Figure 1E. Quadrature detection in t_1 (a, b) and t_2 (b) is obtained with the TPPI or States-TPPI (Marion et al., 1989) method.

resonances visible in (b) and which originate from chemical exchange and dipolar interactions with H_2O are efficiently suppressed in (a). The only two observable peaks in (a) stem from chemical exchange between two OH protons of the protein and H_2O.

Resonance assignments for the bound ligand are obtained with the schemes of Figures 1D and 1E. Ex-

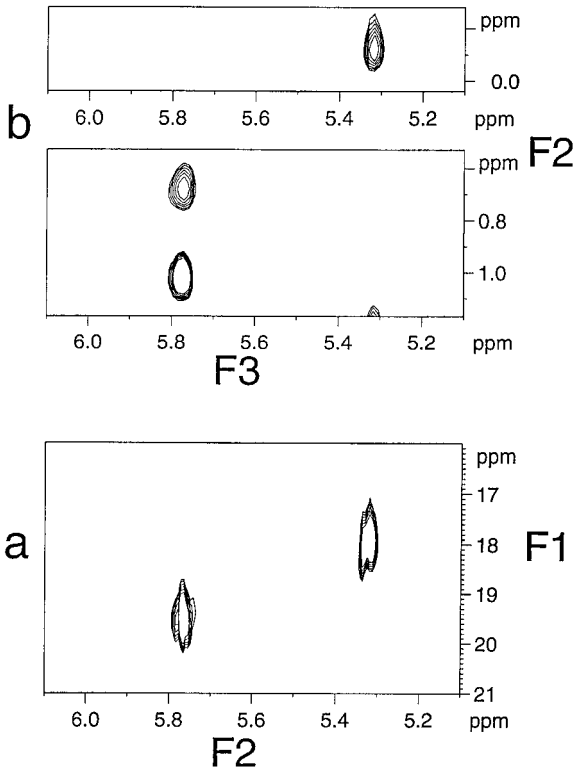

Figure 9. (a) Expanded region from the 2D spectrum of the binary complex recorded with the pulse sequence of Figure 8a (with scheme A). (b) Two $\omega_2(^1H)$-$\omega_3(^1H)$ slices taken at the ω_1 (^{13}C) frequency of the two cross peaks in (a) extracted from the 3D spectrum recorded with the pulse sequence of Figure 8b (with scheme B). The spectrum in (a) was recorded with 256 scans for each of the 220 t_1 increments and with 2048 points for t_2. The spectral width in ω_1 and ω_2 was 148 and 12 ppm, respectively. The repetition time and the mixing time were 1.15 s and 142 ms, respectively. The data were multiplied simply with a cosine window function in both dimensions prior to Fourier transformation. The spectrum in (b) was recorded with 128 scans for each of the 22 t_1 and 64 t_2 increments and with 512 points for t_3. The spectral width in ω_1, ω_2 and ω_3 was 26, 6.4, 6.4 ppm, respectively. The ^1H carrier frequency was set at 2.89 ppm. The repetition time and the mixing time were 0.9 s and 142 ms, respectively. The data were multiplied simply with a cosine window function in all three dimensions. The total measuring time was 19 h for (a) and 52 h for (b).

panded regions of these $^{13}C/^{15}N$ ω_2 half-filter TOCSY and NOESY spectra are shown in Figure 5, upper trace and lower trace, respectively. For unambiguous spin-system assignments the 2D $^{13}C/^{15}N$ ω_2 half-filter PFG DQ experiment was also used (Dalvit et al., 1998). The excellent H_2O and protein resonances suppression in these experiments allowed easy resonance assignment of the ligand. Therefore there is no requirement of preparing additional samples dissolved in D_2O. It should be pointed out that the complete purging of the ^{13}C- and ^{15}N-bound protons results in a narrow diagonal, thus facilitating the observation of connectivities between almost degenerate resonances (see Figure 5).

In addition to the ligand intramolecular NOEs, the protein intramolecular NOEs involving the OH protons and the intermolecular NOEs between ligand and protein are also observed in the spectrum of Figure 5 (lower trace). These NOEs are asymmetric with respect to the diagonal and are observed at the ω_2 frequency of the ligand and protein OH resonances. It is therefore evident that the scheme of Figure 1E can also be used for deriving important distance constraints for the hydroxyl protons of the serine and threonine residues. As seen in Figure 5 both intramolecular and intermolecular protein-ligand NOEs are positive ($\sigma < 0$). The observation of only the ligand intramolecular NOE in a 2D experiment is possible by inserting in the pulse sequence of Figure 1E a $^{13}C/^{15}N$ ω_1 filter scheme. The pulse sequences for the 2D $^{13}C/^{15}N$ ω_2 half-filter NOESY with a ^{13}C ω_1 filter and with a $^{13}C/^{15}N$ ω_1 filter are depicted in Figures 6a and 6b, respectively. The delay τ is equal to $1/(2^1J_{CH})$ where $^1J_{CH}$ has an intermediate value between the aromatic and aliphatic heteronuclear coupling constant values. The $^{13}C/^{15}N$ ω_1 filter element of the scheme of Figure 6b is the same, with the exception of the gradients, to that reported in the literature (Ikura and Bax, 1992). Figure 7 shows an expanded region of the 2D $^{13}C/^{15}N$ ω_2 half-filter NOESY experiment without (a) and with (b) a ^{13}C ω_1 filter. The experiments have been recorded with the pulse sequences of Figures 1E and 6a, respectively. Several NOE cross peaks are observed in Figure 7a between the ligand methyl groups and some protein aromatic resonances. All these NOEs are efficiently removed in Figure 7b and only the ligand intramolecular NOEs are visible.

The $^{13}C/^{15}N$ ω_2 half-filter of Figures 1A and 1B can also be implemented in the 2D and 3D ^{13}C edited HSQC-NOESY experiments. This type of experiments is particularly advantageous when problems of severe overlap are encountered in the proton dimension. The pulse sequences for the 2D and 3D ω_1 ^{13}C edited and $^{13}C/^{15}N$ half-filter (in the acquisition dimension) HSQC-NOESY experiments are depicted in Figures 8a and 8b, respectively. The version of the experiments with ω_1 ^{15}N edited and $^{13}C/^{15}N$ half-filter in the acquisition dimension is obtained from the pulse sequences of Figure 8 by simply interchanging the ^{13}C and ^{15}N pulses before the filter and by setting $\tau/2$ to 2.4–2.7 ms. An expanded region extracted from the 2D spectrum recorded with the pulse sequence of Fig-

ure 8a is displayed in Figure 9a. Two NOEs between two $^{13}CH_3$ groups of the protein and two protons not bound to ^{13}C and ^{15}N are observed in this spectrum. The two $\omega_2(^1H) - \omega_3(^1H)$ slices taken at the ω_1 (^{13}C) frequency of the two cross peaks of Figure 9a from the 3D spectrum recorded with the pulse sequence of Figure 8b (with filter B) are shown in Figure 9b. The downfield cross peak in Figure 9a is the result of two different NOE contributions which originate from two different $^{13}CH_3$ groups having the same ^{13}C frequency. However the two methyl groups have different ^1H chemical shift and therefore the overlap is removed in the $\omega_2\omega_3$ plane of the 3D spectrum as evident in Figure 9b.

Conclusions

In conclusion, it has been shown that the modified $^{13}C/^{15}N$ ω_2 half-filter TOCSY, NOESY and ePHOGSY experiments represent a powerful tool for obtaining resonance assignment, structure determination and hydration properties of a ligand bound to a labelled biological macromolecule.

Acknowledgements

We thank the reviewers for useful suggestions.

References

Bax, A., Grzesiek, S., Gronenborn, A.M. and Clore, G.M. (1994) *J. Magn. Reson.*, **A106**, 269–273.
Baht, T.N., Bentley, G.A., Boulot, G., Greene, M.I., Tello, D., Dall'Acqua, W., Souchon, H., Schwarz, F.P., Mariuzza, R.A. and Poljak, R.J. (1994) *Proc. Natl. Acad. Sci. USA*, **91**, 1089–1093.
Birlirakis, N., Cerdan, R. and Guittet, E. (1996) *J. Biomol. NMR*, **8**, 487–491.
Böckmann, A. and Guittet, E. (1996) *J. Biomol. NMR*, **8**, 87–92.
Braden, B.C., Fields, B.A. and Poljak, R.J. (1995) *J. Mol. Recognition*, **8**, 317–325.
Chuprina, V.P., Rullmann, J.A.C., Lamerichs, R.M.J.N., van Boom, J.H., Boelens, R. and Kaptein, R. (1993) *J. Mol. Biol.*, **234**, 446–462.
Clore, G.M., Bax, A., Wingfield, P.T. and Gronenborn, A.M. (1990) *Biochemistry*, **29**, 5671–5676.
Clore, G.M., Bax, A., Omichinski, J.G. and Gronenborn, A.M. (1994) *Structure*, **2**, 89–94.
Dalvit, C. and Hommel, U. (1995) *J. Magn. Reson.*, **B109**, 334–338.
Dalvit, C. (1996) *J. Magn. Reson.*, **B112**, 282–288.
Dalvit, C., Ramage, P. and Hommel, U. (1998) *J. Magn. Reson.*, **131**, 148–153.
Denisov, V.P., Venu, K., Peters, J., Hörlein, H.D. and Halle, B. (1997) *J. Phys. Chem. B.*, **101**, 9380–9389.
Dötsch, V. and Wider, G., (1995) *J. Am. Chem. Soc.*, **117**, 6064–6070.
Folmer, R.H.A., Hilbers, C.W., Konings, R.N.H. and Hallenga, K. (1995) *J. Biomol. NMR*, **5**, 427–432.
Gemmecker, G., Olejniczak, E.T. and Fesik, S.W. (1992) *J. Magn. Reson.*, **96**, 199–204.
Grzesiek, S. and Bax, A. (1993) *J. Biomol. NMR*, **3**, 627–638.
Hwang, T.-L. and Shaka, A.J. (1995) *J. Magn. Reson.*, **A112**, 275–279.
Hwang, T.-L., Mori, S., Shaka, A.J. and Van Zijl, P.C.M. (1997) *J. Am. Chem. Soc.*, **119**, 6203–6204.
Ikura, M. and Bax, A. (1992) *J. Am. Chem. Soc.*, **114**, 2433–2440.
Keeler, J., Clowes, R.T., Davis, A.L. and Laue, E.D. (1994) *Methods Enzymol.*, **239**, 145–207.
Kogler, H., Sørensen, O.W. and Ernst, R.R. (1983) *J. Magn. Reson.*, **55**, 157–163.
Kriwacki, R.W., Hill, R.B., Flanagan, J.M., Caradonna, J.P. and Prestegard, J.H. (1993) *J. Am. Chem. Soc.*, **115**, 8907–8911.
Lee, J., Fejzo, J. and Wagner, G. (1993) *J. Magn. Reson.*, **B102**, 322–325.
Lee, W., Revington, M.J., Arrowsmith, C. and Kay, L.E. (1994) *FEBS Lett.*, **350**, 87–90.
Marion, D. and Wüthrich, K. (1983) *Biochem. Biophys. Res. Commun.*, **113**, 967–974.
Marion, D., Ikura, M., Tschudin, R. and Bax, A. (1989) *J. Magn. Reson.*, **85**, 393–399.
Mori, S., Johnson, M.O., Berg, J.M. and Van Zijl, P.C.M. (1994) *J. Am. Chem. Soc.*, **116**, 11982–11984.
Mori, S., Berg, J.M. and Van Zijl, P.C.M. (1996) *J. Biomol. NMR*, **7**, 77–82.
Ogura, K., Terasawa, H. and Inagaki, F. (1996) *J. Biomol. NMR*, **8**, 492–498.
Otting, G. and Wüthrich, K. (1989a) *J. Am. Chem. Soc.*, **111**, 1871–1875.
Otting, G. and Wüthrich, K. (1989b) *J. Magn. Reson.*, **85**, 586–594.
Otting, G. and Wüthrich, K. (1990) *Q. Rev. Biophys.*, **23**, 39–96.
Otting, G., Liepinsh, E. and Wüthrich, K. (1991) *Science*, **254**, 974–980.
Otting, G. and Liepinsh, E. (1995) *J. Biomol. NMR*, **5**, 420–426.
Petros, A.M., Kawai, M., Luly, J.R. and Fesik, S.W. (1992) *FEBS Lett.*, **308**, 309–314.
Qian, Y.Q., Otting, G. and Wüthrich, K. (1993) *J. Am. Chem. Soc.*, **115**, 1189–1190.
Renzoni, D.A., Zvelebil, M.J.J.M., Lundback, T. and Ladbury, J.E. (1997) In *Structure-Based Drug Design: Thermodynamics, Modeling and Strategy*, (Eds. Ladbury, J.E. and Connelly, P.R.) Springer-Verlag, Berlin, pp. 161–184.
Shaka, A.J., Keeler, J. and Freeman, R. (1983) *J. Magn. Reson.*, **53**, 313–340.
Sklenár, V. (1995) *J. Magn. Reson.*, **A114**, 132–135.
Sobol, A.G., Wider, G., Iwai, H. and Wüthrich, K. (1998) *J. Magn. Reson.*, **130**, 262–271.
Wider, G., Weber, C., Traber, R., Widmer, H. and Wüthrich, K. (1990) *J. Am. Chem. Soc.*, **112**, 9015–9016.
Wider, G., Riek, R. and Wüthrich, K. (1996) *J. Am. Chem. Soc.*, **118**, 11629–11634.
Zwahlen, C., Legault, P., Vincent, S.J.F., Greenblatt, J., Konrat, R. and Kay, L.E. (1997) *J. Am. Chem. Soc.*, **119**, 6711–6721.